

Available online at [www.sciencedirect.com](http://www.sciencedirect.com)**ScienceDirect**

Procedia Engineering 160 (2016) 183 – 190

**Procedia  
Engineering**[www.elsevier.com/locate/procedia](http://www.elsevier.com/locate/procedia)

XVIII International Colloquium on Mechanical Fatigue of Metals (ICMFM XVIII)

## Short crack behavior during low-cycle fatigue in high-strength bainitic steel

M.C. Marinelli<sup>a\*</sup>, I. Alvarez-Armas<sup>a</sup>, U. Krupp<sup>b</sup><sup>a</sup>*Instituto de Física Rosario – Consejo Nacional de Investigaciones Científicas y Técnicas (CONICET), Universidad Nacional de Rosario, Bv. 27 de febrero 210 bis, 2000 Rosario, Argentina.*<sup>b</sup>*Faculty of Engineering and Computer Science, University of Applied Sciences, Osnabrück, Germany*

---

### Abstract

Nowadays, the most modern bainitic steels are designed with much reduced carbon and other alloying element concentrations exhibiting excellent mechanical properties and are widely applied in industry. However, many engineering components contain a variety of stress concentrators such as grooves, fillets, holes or non-metallic inclusions and these components are exposed to dynamic cyclic loading. It has been observed that fatigue failure usually occurs as a result of crack initiation and growth from these stress raisers. The proposal of this work is to analyze the mechanisms involved in the initiation and propagation of microcracks during low-cycle fatigue in the bainitic steel 16CrMnV7-7. From scanning electron microscopy observations (SEM) in combination with electron backscattered diffraction (EBSD) measurements, the slip systems and their associated Schmid factors are analyzed in the bainitic ferrite blocks and correlated to the short crack path. Moreover, the dislocation structure developed was analyzed and correlated with the formation and propagation of microcracks. The principal results show that the microcracks initiate along slip systems with the highest Schmid factor and that the highly misorientated bainitic ferrite blocks are strong barriers to crack propagation.

© 2016 Published by Elsevier Ltd. This is an open access article under the CC BY-NC-ND license (<http://creativecommons.org/licenses/by-nc-nd/4.0/>).

Peer-review under responsibility of the University of Oviedo

**Keywords:** Low-cycle fatigue; bainitic steel; microcracks nucleation and propagation.

---

---

\* Corresponding author. Tel.: +54 -341 -4853200; fax: +54- 341- 4808584.

E-mail address: [marinelli@ifir-conicet.gov.ar](mailto:marinelli@ifir-conicet.gov.ar)

## 1. Introduction

The high-strength bainitic steels are processed using accelerated cooling in order to obtain the necessary bainitic microstructure. In the bainite transformation, the prior austenite grain is divided into a three-level hierarchy similar to the lath martensite structure in terms of morphology: packet, block and lath. The packet consists of one, or several set of blocks that are individually further subdivided into a group of laths with the same habit plane with respect to the parent austenite and similar orientation [1]. Furthermore, the fine laths of bainitic ferrite are separated by carbon-enriched regions of austenite with or without martensite [2-4]. These steels exhibit excellent mechanical properties and are widely applied in the automobile industry as crash reinforcement bars to protect against sidewise impact and for injection lines (under pulsating loads) in common rail diesel engines [5]. Moreover, many engineering components contain a variety of stress concentrators such as grooves, fillets, holes or non-metallic inclusions and these components are exposed to dynamic cyclic loading. It is well known that fatigue failure usually occurs as a result of crack initiation and growth from these stress raisers. Then, the correct estimations of stress/strain concentration and crack development in the critical region are essential for practical machine design in service cyclic loading. In previous studies, Scanning Electron Microscopy (SEM) has been used to analyze the fracture surfaces, related to the fatigue behavior of the bainitic steels. Branco et al. [6] studied the fatigue damage mechanism of high strength steel after low-cycle fatigue testing and concluded that the microcracks initiate along the slip band on the sample surface and they grow through the grain boundaries and eventually form a coalescence of short cracks, which further coalescence propagates into the bulk perpendicularly to the stress axis. Sankaran et al. [7, 8] revealed that crack initiation occurred at slip band extrusions/intrusions on the surface under mixed mode (ductile and brittle) in multiphase (ferrite/bainite/ martensite) microstructures. Recently, using Electron Backscatter Diffraction (EBSD), Rementería et al. [9] identified the active slip systems in the bainitic ferrite and the crack deflection at grain boundaries in nanobainitic steels with high-carbon (0.67C) and high-silicon (1.67Si). They reported that the crack initiation occurs at the surface during Low Cycle Fatigue (LCF) and the crack initiates on inclusions during High Cycle Fatigue (HCF). Moreover, the results showed that the crack grows along the ferrite slip (110)  $\langle 111 \rangle$  with the highest Schmid factor and that the microstructural features control the crack deflection. A similar study is proposed to analyze the mechanisms involved in the initiation and propagation of microcracks during LCF in the reduced carbon bainitic steel 16CrMnV7-7. Furthermore, from scanning SEM in combination with EBSD measurements, the slip systems and their associated Schmid factors are analyzed in the bainitic ferrite blocks and correlated to the short crack path. Additionally, the dislocation structure developed will be analyzed and correlated with the formation and propagation of microcracks.

### Nomenclature

EBSD	electron backscatter diffraction
HCF	high cycle fatigue
LCF	low cycle fatigue
SEM	scanning electron microscopy
SF	Schmid factor
TEM	transmission electron microscopy
XRD	x-ray diffraction

## 2. Material and experimental procedure

The material considered in this work is the bainitic steel 16CrMnV7-7 with a nominal chemical composition as given in Table 1. The material was supplied by Georgsmarienhütte Steel (Germany) in the form of hot-rolled cylindrical bars of 30 mm in diameter. Optimal material properties are achieved by a controlled cooling down until 350 °C.

Table 1. Nominal chemical composition of the 16CrMnV7-7 (in wt. %).

C	Si	Mn	P	S	Al	Sn
0.15-0.20	0.20-0.30	1.68-1.80	<0.015	0.010-0.020	0.018-0.028	<0.020
Cr	Mo	Ni	V	Nb	N	Cu
0.70-1.80	0.03-0.06	0.12-0.25	0.05-0.15	0.020-0.040	0.018-0.025	<0.20

The fatigue tests were carried out on shallow notched cylindrical specimens. The surface of the shallow notch was mechanically and electrolytically polished using a solution 10% perchloric in ethanol to improve the observation of microcrack nucleation and growth. The central part of the notch was monitored during the test using an in situ optical system consisting of a CCD camera, JAI model CM-140MCL with a 50X objective,  $\pm 1\mu\text{m}$  FD and 13mm WD and a 12X ultra zoom.

Push-pull fatigue tests were performed at room temperature on an electromechanic testing machine INSTRON 1362. The fatigue test were carried out under constant plastic strain amplitude of  $\Delta\varepsilon_p = 0.2\%$  with a fully reversed triangular wave and total strain rate of  $2 \times 10^{-3}\text{s}^{-1}$ .

X-ray diffraction (XRD) analysis was used for the identification and quantification of retained austenite in the as-received steel. XRD tests were performed using a Philips X'Pert Pro MPD diffractometer, equipped with a Cu  $K\alpha$  tube. Damage surface evolution and crack propagation studies were carried out combining SEM observations with EBSD measurements, which was used to determine the distribution of the phases and the crystallographic orientation as well as the size of bainitic ferrite laths and the slip systems. The samples for XRD and EBSD analysis were ground to 2000 grit paper, followed by electro polishing with a solution of 10% perchloric acid and 90% ethanol at  $T = -15\text{ }^\circ\text{C}$ ,  $V = 10\text{ V}$ ,  $I = 1\text{ A}$  and  $t = 4\text{ min}$ .

Internal dislocation structures were studied by transmission electron microscopy (TEM) in a Philips CM 200 transmission electron microscope operated at 160 kV. Thin foils were prepared from slices taken at different depths from the shallow-notched area parallel to the specimen axis. The discs of 3 mm in diameter were subsequently thinned and electro-polished in a twin-jet polishing unit using a 10% perchloric acid and 90% ethanol mixture at  $T = -17\text{ }^\circ\text{C}$  and  $V = 20\text{ V}$ .

### 3. Results

#### 3.1. Microstructure

The constituent phases of the as-received material were analyzed by XRD. Fig. 1 shows the X-ray patterns indicating a 95 Vol. % of bainitic ferrite and 5 Vol.% of retained austenite. The retained austenite was found between blocks and laths of bainitic ferrite as shows the phase map obtained by EBSD in Fig. 2. Moreover, Fig. 3 shows an Inverse Pole Figure (IPF) map and the misorientation distribution of the blocks of bainitic ferrite in the as-received bainitic steel. From this graphic a large proportion of high-angle misorientation between bainitic blocks is observed.

A more detailed study made by TEM has revealed a fine dispersion of cementite precipitates, whose average spacing is of  $0.3\mu\text{m}$ , in the matrix of the bainitic ferrite laths of average width corresponding to  $0.6\mu\text{m}$ . This density of precipitates is relatively low and thus difficult to be detected by XRD.

Fig. 4 shows a bright field and dark field image with the corresponding selected area electron diffraction patterns. The double points in the electron diffraction patterns corresponding to  $\{111\}_\gamma$  and  $\{110\}_\alpha$  planes indicate the coexistence of both austenite and ferrite phases. Moreover, in this dark field image the retained austenite and the cementite precipitation can be clearly observed. Additionally, the bright field image shows a homogeneous distribution of dislocations in the bainitic ferrite as is observed in Fig. 4a.

a

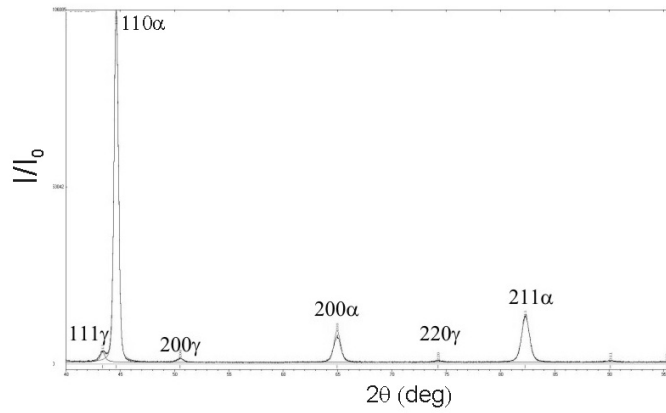


Fig. 1. X-ray patterns indicating a 95 Vol.% of bainitic ferrite and 5 Vol.% of retained austenite.

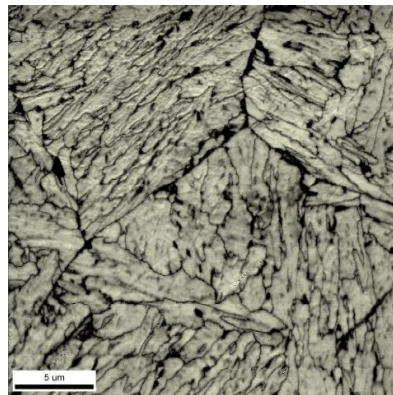
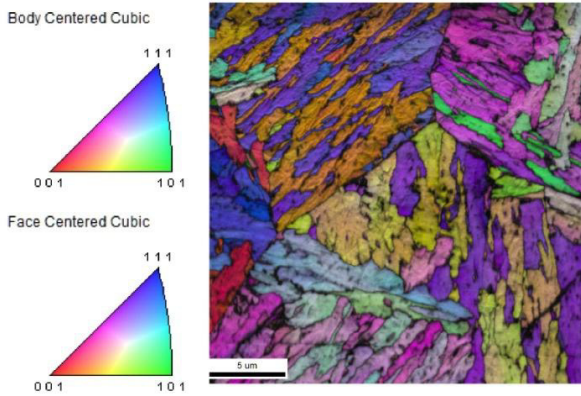


Fig. 2. EBSD map indicating the bainitic steel phases: white for bainitic ferrite and black for retained austenite.

a



b

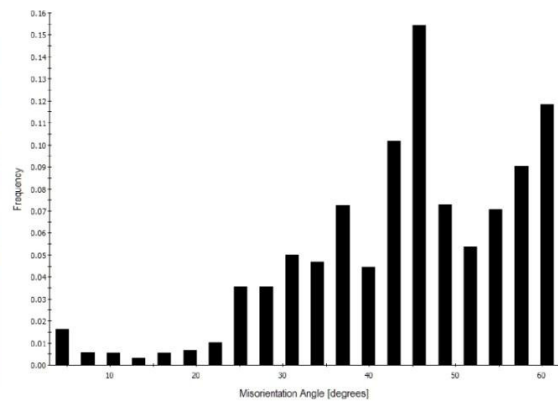


Fig. 3. As received bainitic steel. (a) IPF map; (b) misorientation distribution of bainitic ferrite blocks.

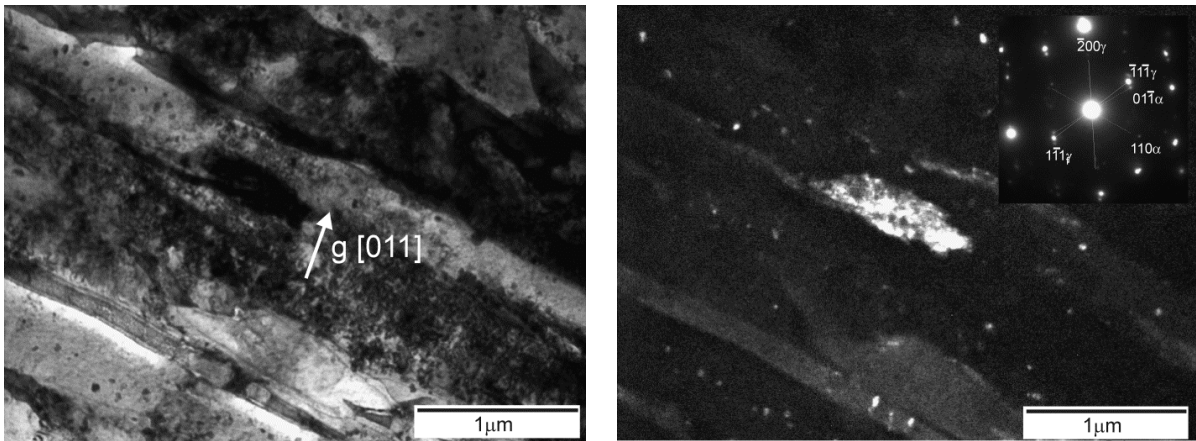


Fig. 4. TEM microstructure of bainitic steel 16CrMnV7-7. (a) bright field image showing lath of bainitic ferrite with a high density of dislocations. (b) Corresponding dark field image (obtained with the double diffraction point:  $(\bar{1}\bar{1}\bar{1})\gamma$  and  $(0\bar{1}\bar{1})\alpha$ ) with electron diffraction patterns showing retained austenite and cementite precipitates

### 3.2. Mechanical behavior

The cyclic behavior of the bainitic steel 16CrMnV7-7 at room temperature under plastic-strain control for  $\Delta\varepsilon_p = 0.2\%$  is shown in Fig. 5. The curve shows a short initial cyclic hardening stage, followed by a continuous cyclic softening that ends in a state of quasi-saturation.

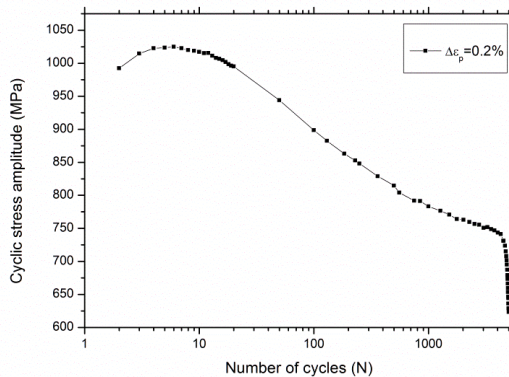


Fig. 5. Cyclic stress amplitude against number of cycles curve of fatigue sample at  $\Delta\varepsilon_p = 0.2\%$ .

### 3.3. Surface damage evolution

In order to analyze the evolution of fatigue damage at  $\Delta\varepsilon_p = 0.2\%$  and the microcracks propagation, the central part of the notch was monitored during the fatigue test. The first slip lines start after 20 cycles (indicated by arrows in Fig. 6b). As cycling proceeds, these lines intensify leading to the microcracks initiation as shown in Fig. 6c (identified as  $f_1$  and  $f_2$ ). Furthermore, it is interesting to note in Fig. 6d an important number of microcracks that remain arrested during cycling (which are indicated by circles) and other microcracks identified as  $f_3$  y  $f_4$  which coalesce into the long crack (Fig. 6 e, f).

Using SEM in combination with EBSD the crystallographic orientations, slip systems and Schmid factor were analyzed. According to this study the microcracks nucleate in the bainitic ferrite laths orientated on slip systems

{110}[111] with the highest Schmid factor. Fig. 7 shows a Schmid factor map obtained by EBSD corresponding to slip systems {110}[111]. In this map it is possible to observe that the microcracks  $f_1, f_3$  and  $f_4$  and those indicated by circles are in the region corresponding with the highest Schmid factor. Moreover, analyzing the slip systems corresponding to  $f_1, f_3$  and  $f_4$  ((110)[ $\bar{1}11$ ] for  $f_1$  and  $f_3$ , and (110)[ $1\bar{1}1$ ] to  $f_4$ ) it is interesting to note that the microcracks share the same (110) plane.

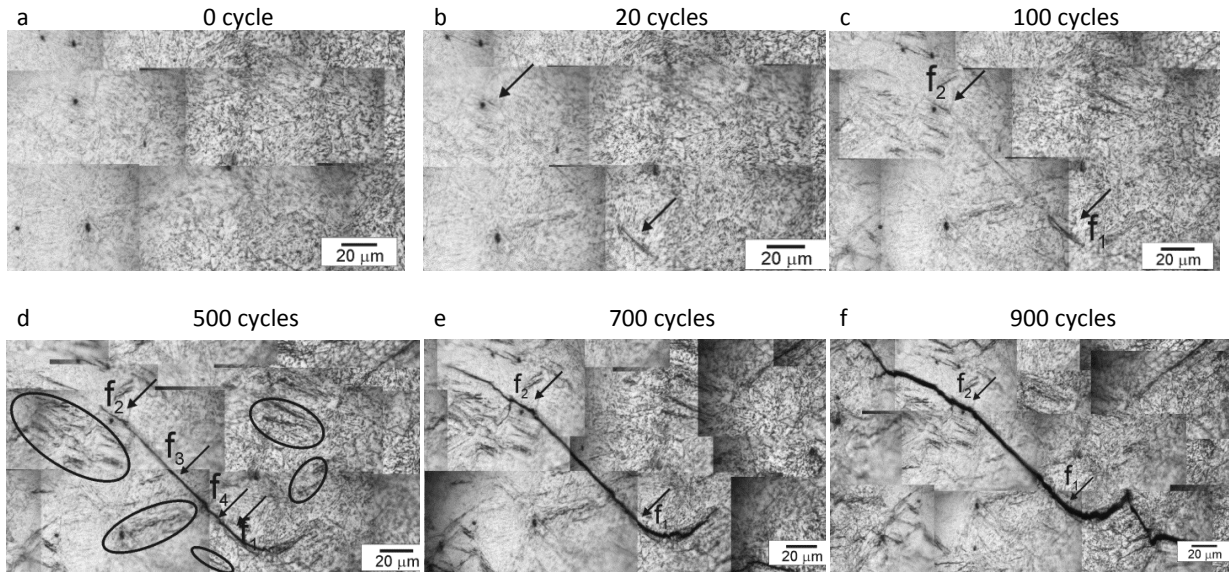


Fig.6. evolution of short crack propagation at  $\Delta\epsilon_p=0.2\%$  .

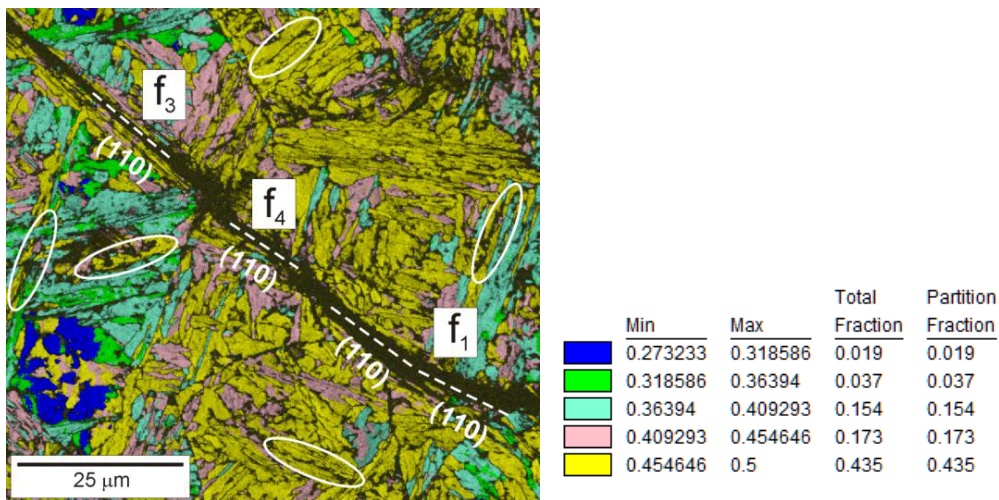


Fig. 7. EBSD Schmid factor map obtained after 900 cycles.

### 3.4 Microstructural evolution

At  $\Delta\varepsilon_p = 0.2\%$ , the characteristic dislocation arrangement in the bulk of the specimen corresponds to heterogeneous distribution of loop patches of dislocations inside the bainitic ferrite laths. Furthermore, it is interesting to note that the phase boundaries (bainitic ferrite / retained austenite) act as barriers against slip transmission into adjacent laths (Fig. 8a). In thin foil taken near the shallow-notched surface a dislocation arrangement in form of cells is observed (Fig. 8b).

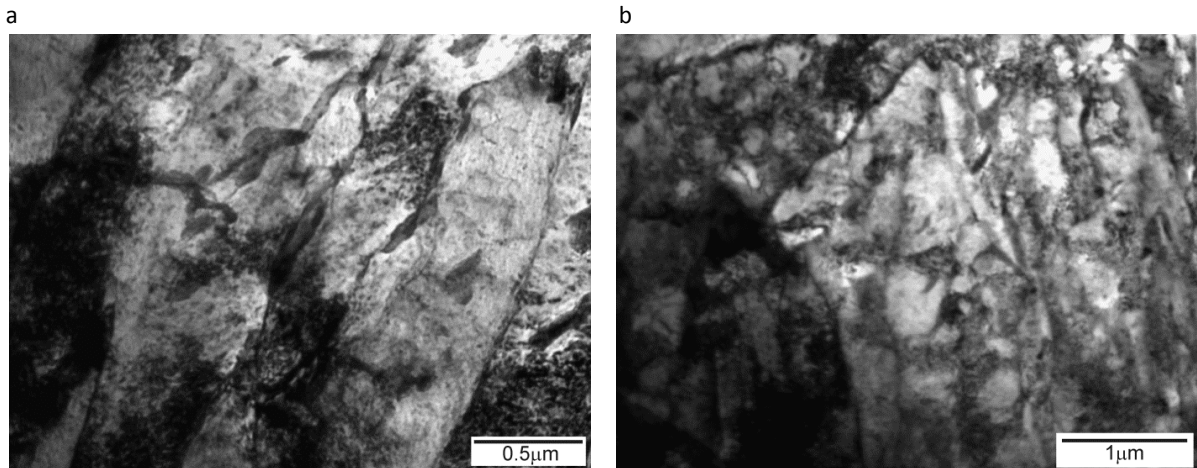


Fig. 8. TEM micrograph of bainitic steel 16CrMnV7-7 fatigued at  $\Delta\varepsilon_p = 0.2\%$ ,  $N=900$  cycles. a) dislocation bundles into the bulk of the specimen, b) dislocation arrangements near the surface of shallow notch

## 4. Discussion

Zhang et al [10] studied the cyclic deformation behavior of the steel with three different bainitic morphologies and analyzed the effects of the bainitic ferrite and the retained austenite on the fatigue behavior. They concluded that the microstructure markedly influences the fatigue behavior of the steel and that the fine bainitic ferrite lath can improve the fatigue strength and then prevent the fatigue crack propagation. Moreover, they argue, according to Kin et al [11] and Diaz et al [12] that the high misorientation angle between two adjacent blocks can modify the crack propagation path and then improve the fatigue life.

In the present study, the misorientation analysis obtained by EBSD in the as received bainitic steel (Fig. 3) revealed that the bainitic ferrite blocks are highly misorientated. This generates strong barriers to the movement of dislocations during cycling and consequently, high localized stress values at the lath boundaries which triggered high localized plastic activity (Fig. 8). Therefore, the microcracks initiate in the bainitic ferrite laths favorably oriented to the stress axis. The Fig. 7 shows that the microcrack grows along the slip systems  $\{110\}\{111\}$  with the highest Schmid factor in the bainitic ferrite laths up to bainite block boundary. If the misorientation between two different crystallographic bainite blocks is high, the cracks remain arrested at boundaries (see for example the crack enclosed in Fig. 7). On the contrary, if there is no change in the active slip planes between bainite blocks, microcracks grow into bainitic ferrite lath of the adjacent block. This fact is illustrated in Fig. 7 where  $f_1$ ,  $f_3$  and  $f_4$  are cracks propagating along the trace of the (110) slip plane. According with Ramenteria et al [9] they proposed that boundaries that are able to deflect the crack are those that delimit blocks, i.e., block boundaries, packet boundaries, twin austenite boundaries or prior austenite boundaries. Therefore, the crystallographic parameter controlling crack deflection would be the bainite block size rather than the bainitic ferrite lath thickness.

## 5. Conclusion

In this paper the study of the mechanisms involved in the initiation and propagation of microcracks during LCF of bainitic steel 16CrMnV7-7 was carried out analyzing the slip systems and their associated Schmid factors in the bainitic ferrite blocks. Moreover, the dislocation structure developed at different depths from the shallow-notched area was analyzed and correlated with the formation and propagation of microcracks. The main conclusions are detailed below:

- The microcracks nucleate in the bainitic ferrite laths along the slip systems  $\{110\}(111)$  with the highest Schmid factor.
- The crystallographic misorientations between bainite blocks and slip planes are parameter controlling crack propagation. If the misorientation between two different crystallographic bainite blocks is high, the cracks remain arrested at boundaries. On the contrary, if there is no change in the active slip planes between bainite blocks, microcracks grow into bainitic ferrite lath of the adjacent block.
- The dislocation structure is more developed near the surface of the specimen than in the bulk, showing heterogeneous distribution of loop patches of dislocations inside the bainitic ferrite laths in the bulk and a dislocation arrangement in form of cells near the surface.

## Acknowledgements

This work was supported by the Bilateral Project between Argentina and Germany CONICET-DFG Res. 992/12 - Consejo Nacional de Investigaciones Científicas y Técnicas – Argentina (CONICET) and Deutsche Forschungsgemeinschaft (DFG).

## References

- [1] H. Beladi, Y. Adachi, I. Timokhina, P.D. Hodgson, Crystallographic analysis of nanobainitic steels, *Scr. Mater.* 60 (2009) 455-458.
- [2] F.G. Caballero, H.K.D.H. Bhadeshia, Very strong bainite, *Curr Opin Solid State Mater Sci.* 8 (2004) 251-7.
- [3] C. Garcia-Mateo, F.G. Caballero, H.K.D.H. Bhadeshia, Acceleration of low-temperature bainite, *ISIJ International.* 43,n°11 (2003)1821-5.
- [4] F.C. Zhang, T.S. Wang, P. Zhang, C.L. Zheng, B. Lv, M. Zhang, Y.Z. Zheng, A novel method for the development of a low-temperature bainitic microstructure in the surface layer of low-carbon steel, *Scr. Mater.* 59 (2008) 294-6.
- [5] F.G. Caballero, M.J. Santofimia, C. Garcia-Mateo, J. Chao, C. Garcia de Andres, Theoretical design and advanced microstructure in super high strength steels, *Mater. Des.* 30 (2009) 2077–83.
- [6] R. Branco, J.D. Costa, F.V. Antunes, Low-cycle fatigue behaviour of 34CrNiMo6 high strength steel, *Theor. Appl. Fract. Mech.* 58 (2012) 28–34.
- [7] S. Sankaran, V. Subramanya Sarma, K.A. Padmanabhan, Low cycle fatigue behavior of a multiphase microalloyed medium carbon steel: comparison between ferrite/pearlite and quenched and tempered microstructures, *Mater. Sci. Eng. A* 345 (2003) 328-35.
- [8] S. Sankaran, V.S. Sarma, S. Sangal, K.A. Padmanabhan. Low cycle fatigue behaviour of a multiphase medium carbon microalloyed steel processed through rolling, *Scr. Mater.* 49 (2003) 503–8.
- [9] R. Rementeria, L. Morales-Rivas, M. Kuntz, C. Garcia-Mateo, E. Kerscher, T. Sourmail, F.G. Caballero, On the role of microstructure in governing the fatigue behaviour of nanostructured bainitic steels, *Mater. Sci. Eng. A* 630 (2015) 71-77.
- [10] F.C. Zhang, X.Y. Long, J. Kang, D. Cao, B. Lv, Cyclic deformation behaviors of high strength carbide-free bainitic steel, *Mater Des.* 94 (2016) 1-8.
- [11] S. Kim, S. Lee, Effect of grain size on fracture toughness in transition temperature region of Mn-Mo-Ni low-alloy steel, *Mater. Des.* 85 (2015) 180-189.
- [12] M. Diaz-Fuentes, A. Iza-Mendia, I. Gutiérrez, Analysis of different acicular ferrite microstructures in low-carbon steels by electron backscattered diffraction, Study of their toughness behavior, *Metall. Mater. Trans. A* 34 (2003) 2505-2516.